Airborne Dust Capture and Induced Airflow of Various Spray Nozzle Designs

Douglas Pollock and John Organiscak

NIOSH, Respiratory Hazards Control Branch, Pittsburgh, Pennsylvania, USA

Water spray characteristics, including droplet size and velocity, airborne dust capture potential, and induced airflow quantity for various spray nozzle designs were evaluated to provide basic information for improving spray applications. Water droplet size and velocity characteristics were initially measured by a Phase Doppler Particle Analyzer (PDPA) for hollow cone, full cone, flat fan, and air atomized spray nozzles at similar operating parameters. Airflow inducement and dust capture experiments were also conducted under the same operating parameters to examine any salient features of the spray nozzle type, droplet characteristics, induced airflow, and airborne dust capture.

Test results indicate that there are trade offs between airflow inducement and dust capture efficiency. A spray nozzle with a wider discharge angle was observed to induce more airflow, but at reduced dust capture efficiencies. Increasing spray nozzle fluid pressure(s) generally reduced water droplet sizes with concurrent increases in droplet velocity, airflow inducement, and airborne dust capture. Placing a three-sided barrier around the spray nozzles normally reduced spray air induction and increased dust capture efficiency. A direct relationship between airborne dust capture efficiency and spray input power normalized per unit of airflow induced was observed. This information can be utilized to improve the performance of water sprays for reducing airborne dust levels.

INTRODUCTION

Water spray dust suppression systems have made significant contributions toward reducing the industry average respirable dust exposure of underground coal miners over an 8-hour shift from over 6 mg/m^3 in 1969 to below 2 mg/m^3 today, which is the standard set by the Federal Mine Safety and Health Administration (MSHA) (NIOSH 1995). However, despite this success, the former Bureau of Mines identified a point of diminishing returns for existing mine spray systems operating at higher supply parameters (pressure and quantity) (Schroeder et al. 1986; Colinet et al. 1991). It was also shown that these

spray systems are probably not adequately providing the dust control needed for meeting lower permissible exposure levels (PEL) enforced by MSHA when silica exceeds 5% (Organiscak et al. 1990). MSHA's coal mine dust PEL is a reduced Mining Research Establishment (MRE) equivalent respirable dust standard of (10 ÷ %quartz) mg/m^3 when there is more than 5% quartz present in the dust sample, as determined by MSHA's P7 infrared method (US CFR 2004; Parobeck and Tomb 2000). MSHA's metal/nonmetal mine PEL is a reduced dust standard of (10 ÷ (%quartz + 2)) mg/m^3 for respirable dust containing at least 1 percent quartz, as determined by NIOSH's X-ray method (US CFR 2004; Parobeck and Tomb 2000). The percentage of airborne coal mine dust samples taken between 1990 and 1999 that exceeds the 2.0 mg/m^3 respirable coal PEL was 8.6%. The percentage of airborne dust samples taken between 1990 and 1999 that exceed the respirable quartz and resulting reduced PEL for coal, metal, and nonmetallic mining were 30.1%, 12.4%, and 7.0%, respectively (NIOSH 2003).

Previous water spray studies have shown differences in airborne respirable dust removal rates for various spray nozzle designs in an enclosed mixing chamber (McCoy et al. 1985). The air-atomized and hollow cone nozzles had higher rates of dust removal per unit of water flow, while the full cone and flat fan had lower removal rates per unit of water flow (USBM 1982). Spray nozzle dust removal rates per unit of water were also found to directly increase with nozzle operating pressures in the confined dust chamber and were recognized to be a product of increased droplet velocity and reduced droplet size.

While high water pressure is advantageous for confined spray dust capture, it can be detrimental to dust capture with unconfined water spray systems commonly used on mining machinery. Laboratory and underground research has shown that as the number of spray nozzles and the water pressure are increased for unconfined spray systems, the dust capture effectiveness per gallon of water is reduced (Schroeder et al. 1986). The improved dust capture from smaller higher velocity droplets at higher spray pressures is offset by the additional dilution from spray induced airflow in the unconfined space (reduced residence time or droplet dust interaction). This research also found that operating unconfined water sprays at high pressures can cause undesirable localized air turbulence, pushing contaminated dusty

air to worker locations (continuous miner rollback) (Jayaraman et al. 1984).

Theoretical models reveal that water spray airborne dust capture efficiency is directly proportional to the relative velocity difference between spray droplets and dust particles and is inversely proportional to droplet diameters (Calvert 1977; Cheng 1973). Cheng modeled that irrespective of droplet velocity 150-μm, 200-μm, and 300-μm diameter droplets have a relative optimum capture efficiency (mostly inertial impaction) on 1-μm, 2-μm, and 3-μm particles, respectively. The current study experimentally examined the effects of spray nozzle design on droplet characteristics, airflow induction, and airborne dust capture efficiency.

SPRAY NOZZLE TYPE AND WATER DROPLET CHARACTERISTICS

To increase the understanding of air inducement and airborne dust capture of different spray nozzle designs, spray droplet sizes and velocities were sampled by using a state-of-the-art laser instrument. NIOSH contracted the measurement of spray nozzle droplet characteristics to the Spray Systems Technology Center (Carnegie Mellon University (CMU), Mechanical Engineering

Dept., Pittsburgh, PA). They utilized a Phase Doppler Particle Analyzer (PDPA) instrument (TSI Inc. Shoreview, MN), which is capable of measuring the size and velocity of water droplets as they pass through the micron-size probe volume of intersecting laser beams. The measurements are based on the principles of light scattering interferometry with an off-axis receiving lens projecting scattered light onto multiple photo detectors. Each detector produces a Doppler burst signal with the frequency proportional to the droplet velocity and the phase shift between the detectors proportional to the droplet size. The PDPA at CMU measured droplet velocities in two directions or axes. A description of the experimental set up and measurements made on spray nozzles can be found in Gemci et al. (2003).

The spray nozzles were mounted on a traversing mechanism so multiple points in the spray pattern could be sampled for droplet characteristics. The spray droplet pattern was sampled at 3 to 4 equally spaced points along a sectional plane 30.48 cm and 60.96 cm perpendicular to the nozzle flow centerline. The spacing of the droplet sampling points varied from 1.27 to 5.08 cm to accommodate various spray pattern angles. The spray pattern was sampled on one side of the nozzle centerline, assuming to be representative of similar radial regions along the plane. Table 1 shows the nozzle designs that were studied for droplet

TABLE 1
Spray nozzles and operating parameters studied

Spray nozzle designation	Nozzle type	Performance specifications	Spray nozzle droplet measurement parameters
*Spraying Systems UniJet Nozzle No. TTD6-45 **81° HC**	Single Fluid Hollow Cone	81° Spray Angle @ 552 kPa & 3.14 lpm	552 & 1103 kPa @ 30.48 cm & 60.96 cm Plane Distances from Nozzle
Spraying Systems UniJet Nozzle No. TTD4-46 **33° HC**	Single Fluid Hollow Cone	33° Spray Angle @ 552 kPa & 2.95 lpm	552 & 1103 kPa @ 30.48 cm & 60.96 cm Plane Distances from Nozzle
Spraying Systems FullJet Nozzle No. GG3 **GG FC**	Single Fluid Full Cone	59° Spray Angle @ 552 kPa & 2.99 lpm	552 & 1103 kPa @ 30.48 cm & 60.96 cm Plane Distances from Nozzle
Spraying Systems UniJet Nozzle No. TT2506 **25° FF**	Single Fluid Flat Spray	31° Spray Angle @ 552 kPa & 3.22 lpm	552 & 1103 kPa @ 30.48 cm & 60.96 cm Plane Distances from Nozzle
Spraying Systems UniJet Nozzle No. TT5006 **50° FF**	Single Fluid Flat Spray	56° Spray Angle @ 552 kPa & 3.22 lpm	552 & 1103 kPa @ 30.48 cm & 60.96 cm Plane Distances from Nozzle
Spraying Systems Air Atomizing Nozzle No. J-SU22 **SU22** Fluid Cap 60100, Air Cap 1401110	Twin Fluid Full Cone	20° Spray Angle @ Air 345 kPa & 150 lpm, Water 276 kPa & 1.77 lpm	172 kPa air/water & 345 kPa air/water @ 1& 2 ft Plane Distances from Nozzle
Spraying Systems Air Atomizing Nozzle No. J-SU42 **SU42** Fluid Cap100150, Air Cap1891125	Twin Fluid Full Cone	21° Spray Angle @ Air 303 kPa & 160 lpm Water 275 kPa & 1.77 lpm	172 kPa air/water & 345 kPa air/water @ 30.48 cm & 60.96 cm Plane Distances from Nozzle

*Mention of any company name or product does not constitute endorsement by the National Institute for Occupational Safety and Health.

Hollow-cone spray pattern

Full-cone spray pattern

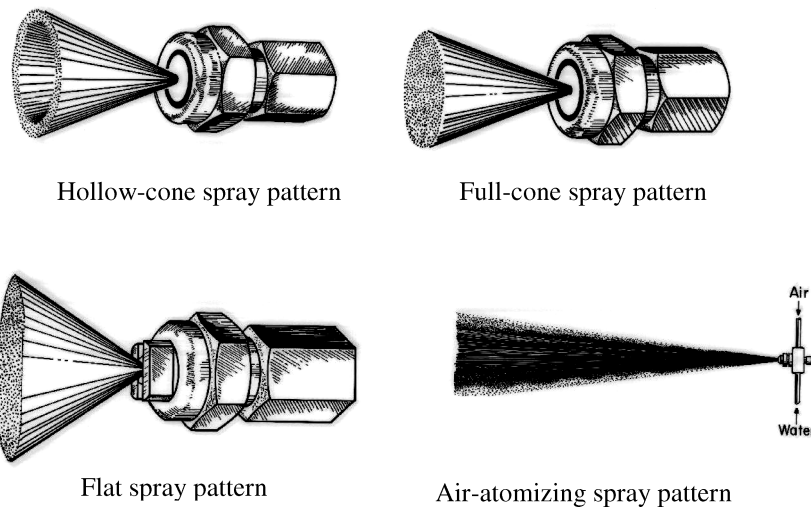Flat spray pattern

Air-atomizing spray pattern

FIG. 1.   Spray nozzles tested.

characteristics by CMU and for air inducement and airborne dust capture by NIOSH. The nozzles chosen for this study are common in the mining industry. Single fluid nozzle designs tested were hollow-cone, full-cone, and flat spray patterns, and they were selected to achieve similar water flow rates at the same operating pressures. Several two-fluid or air-atomizing nozzles in a full cone pattern were also tested. Their water consumption and operating pressures were considerably less than the single-fluid nozzles. Figure 1 shows the types of nozzles tested.

All the spray nozzle designs were sampled at two fluid pressures with water being the medium of droplet formation to examine the droplet characteristics with respect to fluid pressure.

Figure 2 shows the Sauter Mean Diameter (SMD) and mean droplet velocity (parallel to the nozzle axis) measurement results for the second nozzle listed in the table (33° hollow-cone spray) one foot away from the nozzle. SMD represents the mean diameter ratio of total droplet volume to total droplet surface area of the water droplets sampled. The actual droplet sample measurements were made at the points connected by the solid lines,

which were asymmetrically projected to the other side of the spray centerline.

Figure 2 illustrates that this hollow-cone spray nozzle generates smaller water droplets (as defined by SMD) near the center of the hollow cone spray pattern, with larger droplet sizes generated away from the nozzle centerline. In contrast, the mean droplet velocities (parallel to the nozzle axis) are the highest at the spray pattern center with lower droplet velocities generated away from nozzle centerline. Another salient feature observed from these spray droplet characteristics is that higher water spray pressures consistently decrease SMDs and increase mean droplet velocities across the spray pattern. The other spray nozzles tested (full cone, flat fan, and air-atomizing) also exhibited relatively higher droplet velocities at the center of the spray pattern, but differed from the hollow cone nozzle by having relatively larger droplet sizes located at the center of the spray pattern. A concise comparison of the different spray nozzle test data is illustrated in Figures 3 and 4.

Figures 3 and 4 show the range of water droplet SMDs and mean velocities measured across all the spray patterns at both planar distances from the nozzle and operating pressures as specified in Table 1. P1 represents the lower test pressure (552 kPa water nozzles and 172 kPa air-atomized nozzles) and P2 represents the higher test pressure (1,103 kPa water nozzles and 345 kPa air-atomizing nozzles) for each nozzle. The vertical lines within each bar range represent the average centerline SMD and mean velocity for both planar distances measured. As these figures show, higher spray nozzle fluid pressure generally reduces droplet sizes (SMD) and increases mean droplet velocities within the spray pattern. It is also evident from these figures that there are different droplet characteristics with regard to nozzle design or type. The hollow cone nozzles, especially the wider angle nozzle, tend to generate smaller and slower velocity droplets, while the flat fan nozzles tend to generate larger droplet sizes at moderate velocities. On the other hand, the full cone
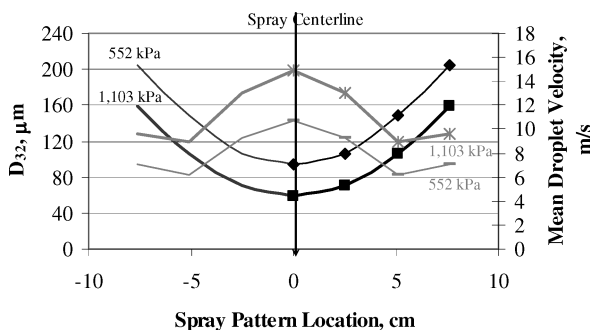

FIG. 2.   Spray droplet characteristics 30.48 cm away from the 33° Hollow-Cone Nozzle. SMD curves are the darker lines. The lighter lines represent the mean droplet velocity. Line thickness represents the water pressure differences.
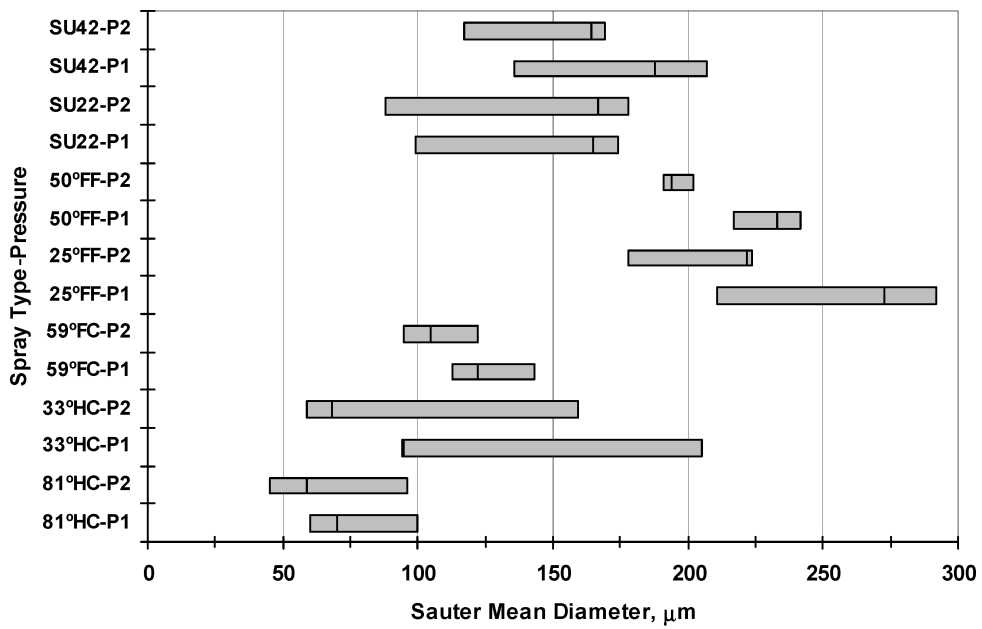
FIG. 3. Sauter Mean Diameter ranges measured within various nozzle spray patterns. The vertical line in each SMD range bar indicates the average centerline SMD for both planar distances measured.

(water only and air-atomizing) nozzles tend to generate droplet size ranges between the hollow-cone and flat fan spray nozzles, with noticeably higher mean droplet velocities generated from the air-atomizing sprays. These general spray droplet characteristics are useful for understanding the differences in spray-induced air movement and dust capture effectiveness, which are measured and discussed below.

SPRAY INDUCEMENT AIR MEASUREMENTS

An open-ended test duct was constructed from plywood to determine the airflow quantity generated by each spray configuration in a some what unrestrictive spray environment. The duct dimensions were 91.44 cm wide by 91.44 cm high by 121.92 cm long. The test spray nozzle was mounted 20.32 cm from the opening on the centerline axis. A hot-wire anemometer with
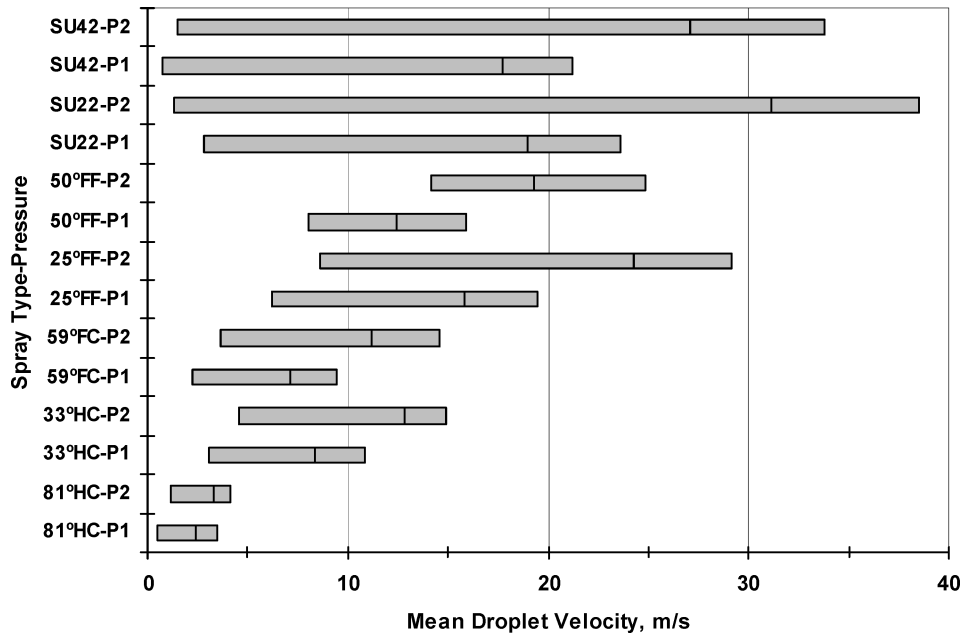

FIG. 4. Mean droplet velocity ranges measured within various nozzle spray patterns. The vertical line in each velocity range bar indicates the average centerline mean velocity for both planar distances measured.
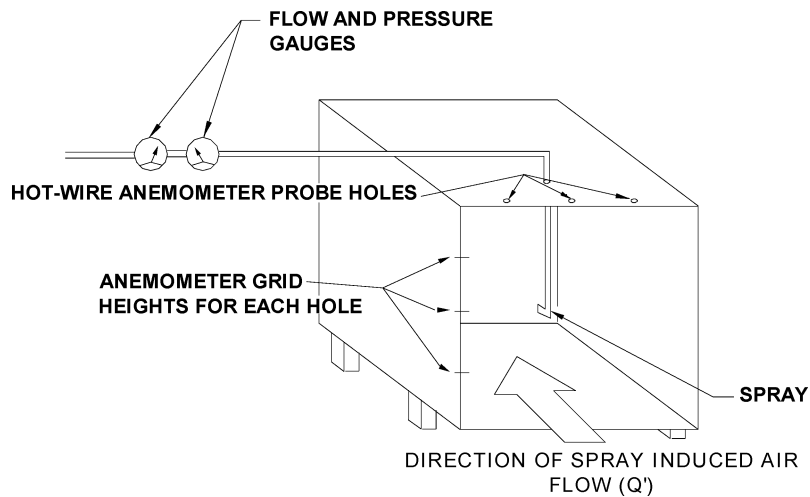
FIG. 5. Air velocity test duct.

statistical capabilities (VelociCalc model 8346 manufactured by TSI Incorporated, Shoreview, MN) was used to take air velocity measurements along a nine-point traverse just upstream of the spray nozzle inside the duct as shown in Figure 5. Each spray nozzle was tested in the test duct to determine the airflow rate induced by the spray. Water pressures were set similar to droplet measurements at 552 kPa and 1,103 kPa while air velocity measurements were taken. For the air-atomizing sprays (Spraying Systems No. J-SU22 and No. J-SU42), the water/air pressures were set at 172 kPa and 345 kPa.

Spray barriers were constructed and mounted under the sprays and flow measurements were taken with the same pressures as listed above. The barrier arrangements consisted of platforms that were 30.48 cm wide × 15.24 cm long, 30.48 cm wide × 30.48 cm long, 15.24 cm wide × 91.44 cm long, and 30.48 cm wide × 91.44 cm long, with removable sides mounted 15.24 cm and 5.08 cm under the spray centerline. The barrier sides were the same dimensions as the corresponding platform (see Figure 6).
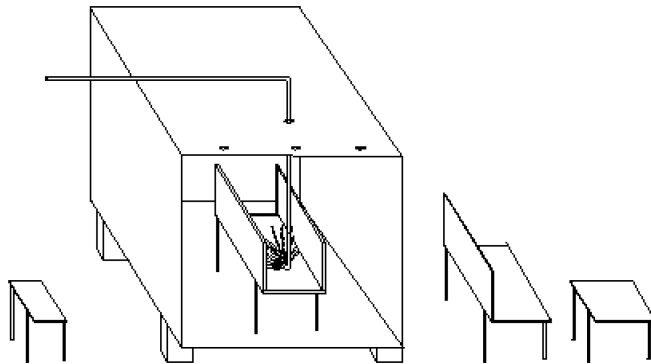

FIG. 6. Air velocity test duct with barriers.

Induced air flow measurements were taken for all spray types while varying the water pressure, barrier size, and location under the spray centerline and installing sides on the barrier. Pressure versus induced airflow curves were generated for each scenario and the data from the airflow curves was utilized in the dust capture experiments for the efficiency calculations of the sprays. More specifically, the airflow curves generated from the barrier arrangements were analyzed to determine the most advantageous arrangement for the dust capture tests.

It should be noted that the airflow inducement measurements were utilized for ranking purposes only. To accurately measure the airflow within this cross section of duct, it would have to be approximately 10 m long upstream of the spray. Due to space limitations and purpose for these measurements, the test duct utilized for these airflow ratings was sufficient for this work. The relative low power provided by the nozzles at the test pressures would have to overcome the additional restriction from static pressure losses associated with a 10 m duct. The purpose of this portion of the study was to investigate the relative performance of the individual spray nozzles under similar operating conditions in a somewhat unrestrictive spray environment.

LABORATORY DUST CAPTURE EXPERIMENTS

The spray dust capture efficiency testing was conducted in a 2.44 m high by 2.44 m wide by 2.44 m deep dust chamber. Dust chamber experiments were conducted for each water spray both with and without barrier arrangements to determine the capture efficiency for each arrangement. Dust was introduced into the chamber by an air inductor until the concentration reached a desired ceiling. A 1.1 m^3/s mixing fan in the chamber was used to disperse the injected dust throughout the chamber before the test. Airborne dust capture efficiency of the sprays was determined by the removal rate of a known concentration of dust in a known volume of the chamber over the application time period. The

dust spray removal rate or capture efficiency was determined by the following equation (Ruggier et al. 1983; McCoy et al. 1985):

$$V \frac{dC}{dt} = -C(Q + F)$$

Which is solved and reduces to:

$$F = \eta Q' = \frac{-V}{t} \ln\left(\frac{C}{C_o}\right) - Q$$

Where:

C–Final Dust Concentration, mg/m^3

C_o–Initial Dust Concentration, mg/m^3

Q–Ventilation flow through Test Chamber added from compressed air in air-atomizing sprays, m^3/s

V–Fixed Volume of Test Chamber, m^3

t–Time, s

F–Dust Removal Mechanism(s), m^3/s

$\eta\, Q'$–Spray Dust Removal or Cleaned Airflow Rate, m^3/s

Q'–Ventilation Flow through Spray Induction, m^3/s

η–Dust Capture Efficiency,%

The dust removal rate ($F = \eta Q'$) was primarily the only mechanism of significance assumed during water spray testing with an additional air dilution mechanism occurring inside the chamber (Q) during air-atomizing testing.

For each test, Keystone Mineral Black 325 BA (Keystone Filler and Manufacturing Co., Muncy, PA) was introduced to reach a level of just over 100 mg/m^3 measured by an instantaneous, real-time aerosol monitor (RAM-1, MIE, Inc., Bedford, MA). The Keystone Mineral Black 325 BA is bituminous coal dust with a size distribution of 100% less than 44 μm and 65% less than 10 μm. The RAM-1 was operated at 2.0 L/min with a Dorr-Oliver 10 mm nylon cyclone to measure the respirable size fraction of dust. When the instantaneous, real-time concentration naturally decayed to 100 mg/m^3, two personal MSA coal mine dust samplers were run for a 3-minute interval to determine the initial average respirable gravimetric dust concentration for calibrating the RAM-1 dust concentration at the beginning of the spray decay (C_o). The MSA coal mine dust sampler consisted of a MSA Elf personal pump calibrated to 2.0 L/min, which was connected to a Dorr-Oliver 10-mm nylon cyclone to capture the respirable fraction of the airborne dust on a MSA coal mine pre-weighed filter cassette. After the 3-minute interval, the spray was operated for a time period required to reduce the RAM-1 dust concentration to around 30 mg/m^3. At this point, the water supply to the spray was shut off and another set of personal MSA coal mine dust samplers were run for a 10-minute period to determine the final average respirable gravimetric dust concentration for calibrating the RAM-1 dust concentration (C) at the end of the spray decay.

The spray dust capture efficiency performance configurations tested in the chamber were conducted by using the same water pressures used while testing the air flow characteristics in the
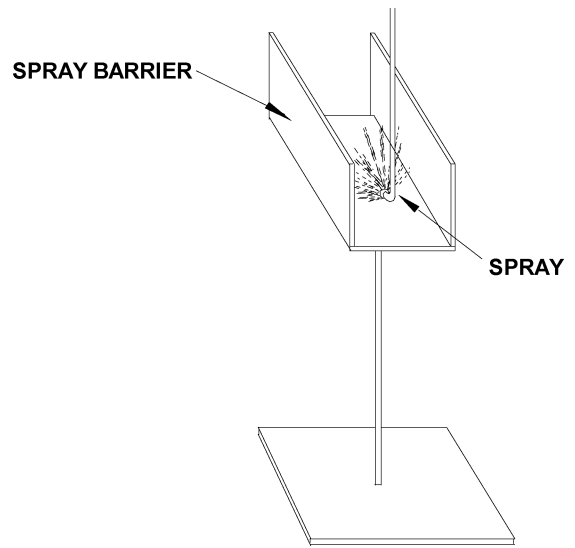

FIG. 7.   Three-sided barrier set-up.

open-ended test duct. This allowed the testing of the sprays at the predetermined air flow rate of the sprays (Q'). For the air atomizing nozzles (Spraying Systems No. J-SU22 and No. J-SU42), the water/air pressures were set at 172 kPa and 345 kPa.

Three repetitions were randomly conducted for each spray at each pressure. During the testing, data (RAM-1 concentration, water pressure, and water flow rate) was continuously recorded using a Telog model 3307 data acquisition system (Telog Instruments, Inc., Victor, NY).

A testing series was then randomly repeated after placing a barrier around the spray, which consisted of a plywood channel 30.48 cm wide by 91.44 cm long with 30.48 cm sides, approximately 15.24 cm below the centerline of the spray (see Figure 7). This barrier arrangement was chosen based on the larger range of airflow changes observed during airflow velocity testing. The airflow quantity changes encountered using this barrier arrangement typically increased by 0.236 m^3/sec. From the increase in water pressure. The dust capture testing was performed in the same method as the unconfined sprays.

Background dust removal mechanisms of the dust chamber itself were also tested and showed that there was about 1% removal efficiency. This was determined by thoroughly wetting the interior of the dust chamber, injecting the dust, and mixing with the 1.1 m^3/s mixing fan (no spray operating) over the same time length of time that the spray tests were performed. After three replications were conducted, the background dust chamber removal mechanisms were considered negligible in these spray efficiency determinations.

AIRFLOW INDUCEMENT AND DUST CAPTURE RESULTS

Figures 8 and 9 show the average spray nozzle test results for the airflow induced and dust capture efficiency in the unconfined
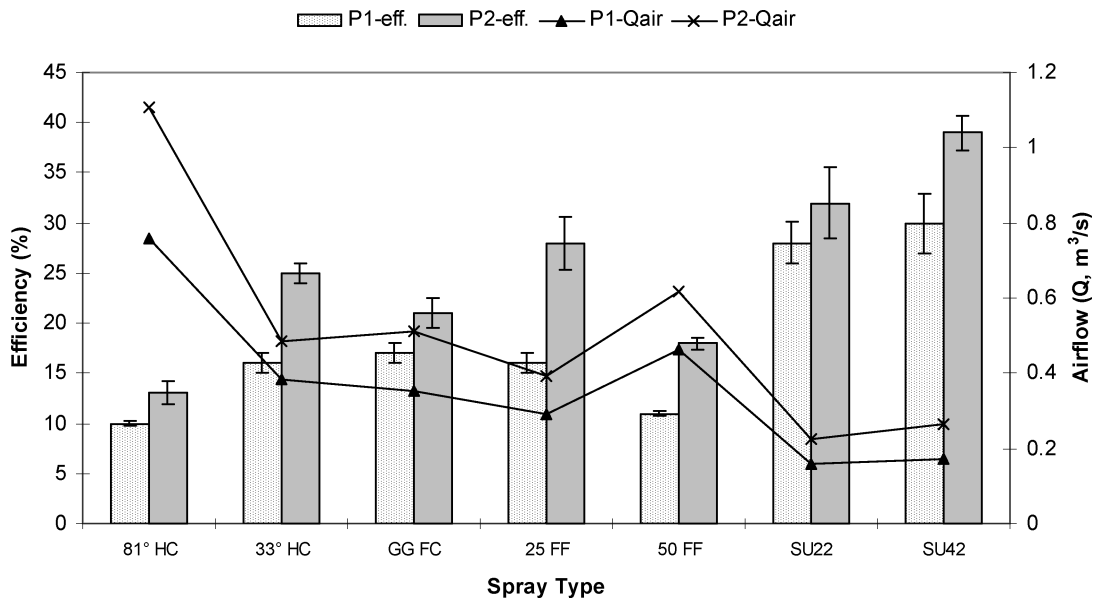
FIG. 8. Dust capture efficiency and airflow for unconfined sprays.

and barrier configurations, respectively. Variations in dust capture experiments are shown by standard deviations (three test repetitions).

Analyzing the sprays according to airflow inducement shows that the 81° HC (Spraying Systems UniJet Nozzle No.TTD6-45) was the best air mover with the air atomizing nozzles (Spraying Systems Air Atomizing Nozzles No. J-SU22 and No. J-SU42) at the lower end of the airflow inducement scale. The discharge angle in the unconfined spray tests seemed to have a direct as-

sociation with the airflow induced. The discharge angles of the sprays specified in Table 1 can be compared to the airflow inducement (Q) shown in Figure 8. The larger angled water sprays, such as the 81°HC, 50° Flat Fan, 59° Full Cone (GG FC), and the 33° HC sprays, induced higher airflows as compared to the 25° Flat Fan water spray and air-atomizing nozzles with discharge angles of around 20°. These airflow induction effects can be attributed to the larger spray discharge angle, which acts to move a larger cross-sectional area of air. Also, the wider angle spray
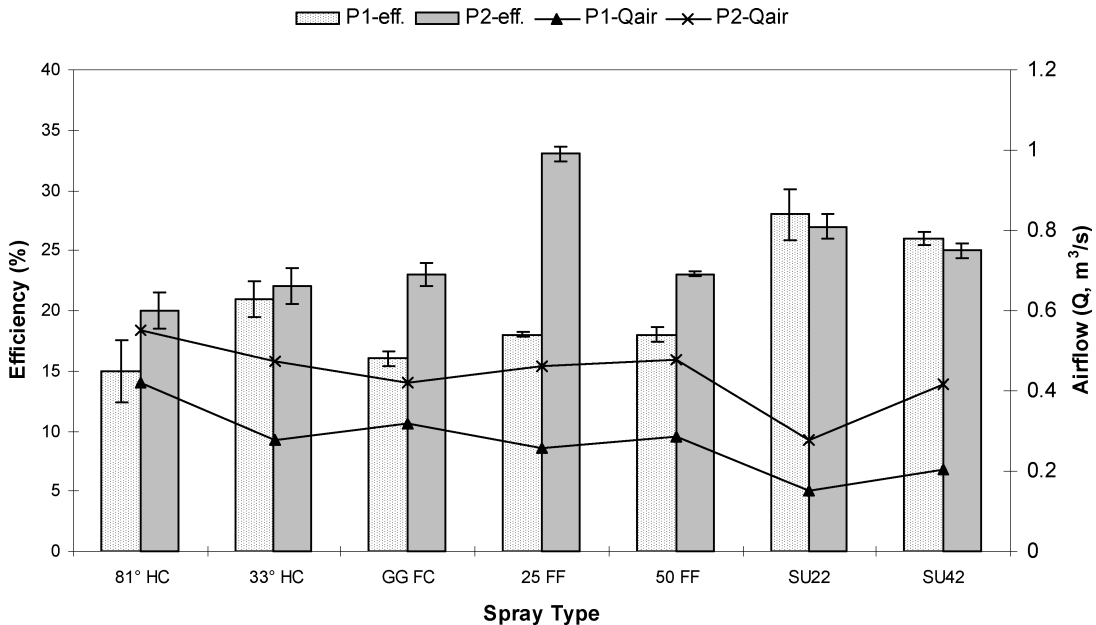

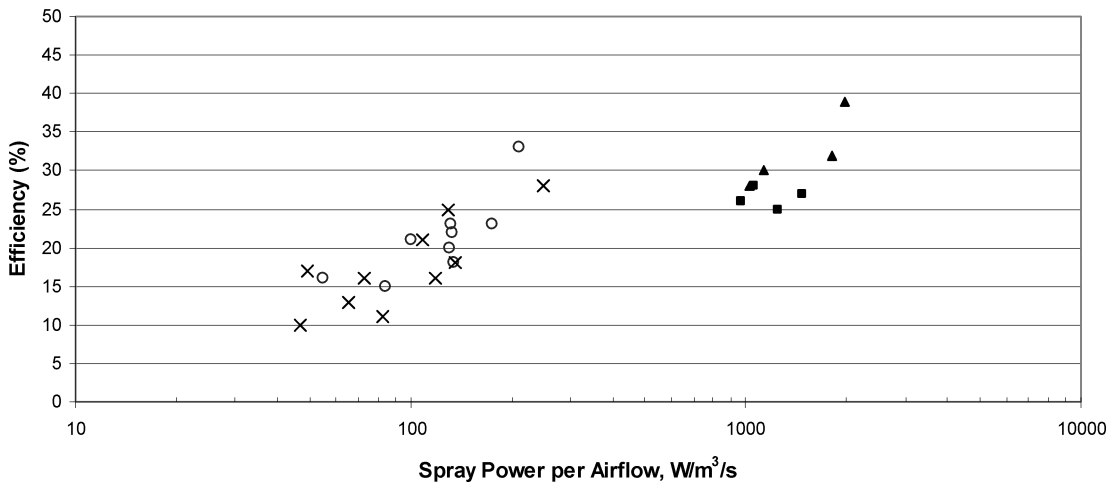FIG. 9. Dust capture efficiency and airflow for sprays with barriers.

FIG. 10.   Spray power and efficiency relationship.

nozzles tended to generate smaller water droplets with more air-to-droplet surface area interaction. The $81°$ HC spray appeared to generate the smallest droplet sizes at the lowest droplet velocities and was the best spray nozzle for moving air as compared to the other sprays. The narrow angle, full cone, air-atomizing sprays had noticeably less air induction than the other sprays, but also had less water mass flow rates for droplet-to-air momentum transfer.

Figures 8 and 9 also show a direct relationship between water pressure and air flow quantity. If the pressure to the spray increases, the airflow rate increases. An increase of water pressure results in an increase of droplet velocity and a decrease in droplet size (see Figures 3 and 4). Smaller and faster droplets impart their increased kinetic energy to the air, inducing more airflow. The addition of the three-sided barrier around the spray decreased the airflow mostly on the wider angled sprays (greater than $25°$), as seen in Figure 9. This can be attributed to the droplets colliding with the barrier sides, and thus losing their energy. Increasing the pressure to the water spray also increases the dust capture efficiency with the exception of the air-atomizing SU22 and SU42 sprays during the testing with the three-sided barrier. A slight air-atomizing dust capture efficiency decrease was only observed for spray fluid pressure increases on the three-sided barrier tests. This reduced efficiency was accompanied by relatively higher induced airflows achieved with the barrier when using the narrower angle, air-atomizing nozzles.

The dust capture efficiency of the spray types appears to compare inversely to the airflow inducement. When the airflow inducement is high, the airborne dust capture efficiency appears to be low. While high airflow inducement may redirect the dust cloud by acting as a spray fan to sweep the dust cloud away from the area, the relatively lower velocity difference between the droplet and the air stream likely diminishes droplet/dust impaction processes in dust removal. Sprays seem to have either high air-moving characteristics or dust removal capability. There are sprays such as the flat fan sprays that offer medium air movement and dust removal capability, as shown in Figure 8. Figure 9 also shows that barrier configurations inversely changed spray airflow and dust capture measurements.

The average spray power input during the dust experiments was normalized by the airflow induction previously measured in the duct at those spray conditions to examine the dust capture efficiency of all of the sprays in more comprehensive terms. The power input is the product of the water flow rate and the water pressure delivered to the spray. In the case of the air-atomizing sprays, the power input is the sum of the water power input plus the air power input to the spray. The water and compressed air equations used to determine the power input can be found in the appendix (Glover 1996). The average dust capture efficiency relationship to the airflow normalized spray power inputs are shown in Figure 10.

Figure 10 indicates that a general direct logarithmic relationship exists between the spray power per airflow induced and the capture efficiency during the spray testing. It also illustrates the trade-offs of dust capture efficiency versus airflow inducement. A spray operating at relatively higher power input per airflow inducement has high dust capture efficiency. On the other hand, sprays operating at the lower end of the chart have relatively lower power input per airflow inducement. These spray types are more air movers than dust capturers, and, therefore, the dust capture efficiency is low. Figure 10 also shows a similar dust capture effect with the barrier. The barrier commonly reduces airflow induction, which usually results in an increase in dust capture efficiency. These trade-offs exist when a spray is impeded by the barrier; there is a reduction in airflow, but a slight increase in dust capture efficiency.

The operation of the air-atomizing nozzles requires not only water but also compressed air to atomize the fluid. Figure 10

TABLE 2
Nozzle spray power per airflow values

Spray nozzle designation	Spray power per airflow (W/m³/s) unconfined P1 P2	Spray power per airflow (W/m³/s) barrier P1 P2
81° HC	47	84
	65	131
33° HC	73	101
	129	133
GG FC	49	55
	108	132
25° FF	119	134
	249	210
50° FF	83	134
	136	176
SU22	1030	1057
	1804	1471
SU42	1129	963
	1983	1254

shows the efficiency of the atomizing nozzles comes with the cost of power input by the water plus the large power input to compress the air to atomize the water.

Table 2 lists the spray nozzle power per airflow values for nozzle design comparison purposes. The values were calculated using the airflow inducement measurements, water and air pressures and water flow rates measured throughout the testing. While the spray power can be more accurately determined from pressures and fluid flow rates taken with calibrated instruments, the spray inducement air measurements had some known inaccuracies from using a short test duct. However, these spray induced airflow measurements were made under similar test conditions and expected to provide relatively good comparisons between sprays.

CONCLUSIONS

Laboratory testing of several water spray nozzle designs show that water supply pressure, spray design, and barriers near the spray can affect the airflow inducement and dust capture efficiency of the spray. Increasing water pressure to the sprays reduces water droplet sizes and increases the droplet velocities, the airflow induction for both unconfined and barrier spray arrangements and the dust capture efficiency of the spray with the exception of the air-atomizing SU22 and SU42 sprays with the three-sided barrier.

The spray nozzle designs with the wider nozzle angles tend to reduce water droplet sizes and droplet velocities. The flat fan nozzles tend to produce the largest water droplet sizes and the air-atomizing sprays tend to generate the highest droplet velocities. Spray designs with a large discharge angle will induce higher airflows compared to sprays with smaller discharge angles op-

erating at the same pressure. A trade-off exists between airflow inducement and dust capture efficiency: spray designs that generate high airflow inducement tend to have low dust capture efficiency, while sprays with high dust capture efficiency tend to have low airflow inducement. Barriers placed around the spray will reduce the airflow induction of the spray while increasing the dust capture efficiency of the spray.

Lastly, a direct relationship was also observed between spray power input per unit airflow versus dust capture efficiency. The sprays with the air moving capability were poor performers for dust capture efficiency, and those with poor airflow inducement had high dust capture efficiency. Also, the addition of barriers caused a reduction in airflow rate and an increase in efficiency.

Based upon the information of spray nozzle performance characteristics obtained through this testing, NIOSH is developing water-powered scrubbers and spray systems to be tested for dust control performance in multiple mining applications.

REFERENCES

Calvert, S. (1977). Scrubbing. In *Air Pollution*, Vol. IV, A. C. Stern (Ed.). Academic Press, New York.

Cheng, L. (1973). Collection of Airborne Dust by Water Sprays, *Ind. Eng. Chem. Process Des. Develop.* 12:221–225.

Colinet, J. F., McClelland, J. J., and Jankowski, J. A. (1991). Interactions and Limitations of Primary Dust Controls for Continuous Miners. Bureau of Mines Report of Investigations, RI 9373, 24 pp.

Gemci, T., Chigier, N., and Organiscak, J. A. (2003). Spray characterization for Coal Mine Dust Removal. Presented at 9th International Conference on Liquid Atomization and Spray Systems (ICLASS 2003), July 13–17, Sorrento, Italy, Chapter 15–1 in Proceedings, 8 pp.

Glover, T. J. (1996). Pocket Ref, Sequoia Publishing, Littleton CO, pp. 11, 426.

Jayaraman, N. I., Kissell, F. N., and Schroeder, W. E. (1984). Modify Spray Heads to Reduce the Dust Rollback on Miners. *Coal Age*, June, 56–57.

McCoy, J. F., Schroeder, W. E., Rajan, S. R., Ruggieri, S. K., and Kissell, F. N. (1985). New Laboratory Measurement Method for Water Spray Dust Control Effectiveness, *Am. Ind. Hyg. Assoc. J.* (46), 735–740.

National Institute for Occupational Safety and Health (NIOSH). (2003). Work-Related Lung Disease Surveillance Report 2002. DHHS (NIOSH) Publication 2003-111.

National Institute for Occupational Safety and Health (NIOSH). (1995). Criteria for a Recommended Standard: Occupational Exposure to Respirable Coal Mine Dust. DHHS (NIOSH) Publication 95-106.

Organiscak, J. A., Page, S. J., and Jankowski, R. A. (1990). Sources and Characteristics of Quartz Dust in Coal Mines. Bureau of Mines Information Circular, IC 9271.

Parobeck, P. S., and Tomb, T. F. (2000). MSHA's Programs to Quantify the Crystalline Silica Content of Respirable Mine Dust Samples. Presented at the 2000 SME Annual Meeting and Exhibit, February 28–March 1, Salt Lake City, Utah, Pre-Print 00–159.

Ruggieri, S. K., Muldoon, T. L., Schroeder, W., Babbit, C., and Rajan, S. (1983). Optimizing Water Sprays for Dust Control on Long Wall Shearer Faces, U.S. Bureau of Mines Final Contract Report, Contract No. J0308019, Foster-Miller, Inc., Waltham, MA, NTIS No. PB 86-205408, 156 pp.

Schroeder, W. E., Babbitt, C., and Muldoon, T. L. (1986). Development of Optimal Water Spray Systems for Dust Control in Underground Mines. Bureau of Mines Final Contract Report, Contract H0199070, Foster-Miller, Inc.

U.S. Bureau of Mines (USBM) (1982). Technology News 150: Dust Knockdown Performance of Water Spray Nozzles. Pittsburgh, PA: U.S. Department of the Interior, Bureau of Mines.

U.S. Code of Federal Regulations. (2004). Title 30—Mineral Resources; Chapter I—Mine Safety and Health, Parts 56 through 58; Subchapter O-Coal Mine Safety and Health, Parts 70 through 74, U.S. Gov. Printing Office, Office of Federal Regulations, July, 2004.

APPENDIX

This appendix contains fluid power equations (at standard barometric pressure and air density).

Spray Power per airflow (P_{sprays}/Q'):

Spray power (P_{sprays}) per airflow for conventional sprays is equal to $(p_{water})(Q_{water})/Q'$

where

p_{water} is the gage pressure (Pascals),

Q_{water} is the water flow rate (m^3/sec) and

Q' is the ventilation flow through spray induction (m^3/s).

For the air-atomizing sprays, $P_{sprays}=P_{water}+P_{air}$

where

P_{water} is the hydraulic power (watts) $= ((p_{water})(Q_{water}))$

and

P_{air} is the theoretical power (watts) to compress the air at standard conditions.

$$P_{air} = 357{,}943(Q_{air})\left[\left(\frac{p_{air}}{101{,}353}+1\right)^{0.283} - 1\right]$$

where

p_{air} is the gage pressure of the air to the nozzle in Pascals

and

Q_{air} is the atomizing air flow rate to the nozzle in m^3/sec.